Struct Chem (2016) 27:557–571
DOI 10.1007/s11224-015-0585-9

ORIGINAL RESEARCH

Effects of the HCN adsorption on the structural and electronic parameters of the beryllium oxide nanotube

Mina Marvi[1] · **Heidar Raissi**[1] · **Hamideh Ghiassi**[1]

Received: 17 January 2015 / Accepted: 18 March 2015 / Published online: 22 April 2015

Abstract The adsorption behavior of the HCN on the surface of beryllium oxide nanotube (BeONT) is studied by the density functional theory. Geometrical parameters, electronic properties and adsorption energies have been calculated for the BeONT and fourteen different HCN configurations on the nanotube. According to the obtained results, the process of the HCN molecule adsorption on different sites on the external surface of the nanotube is exothermic and all of the configurations are stable, while the process of HCN molecule adsorption on the internal surface of the BeONT is endothermic. The adsorption energy values indicate that the HCN molecule can be physically adsorbed on the surface of the BeONT. Furthermore, the HOMO–LUMO gap (Eg) of the BeONT decreases upon the HCN adsorption, resulting in the enhancement of the electrical conductivity. The AIM theory has been also utilized to analyze the properties of the bond critical points: their electron densities and their Laplacians. NBO analysis indicates that the HCN molecule can be adsorbed on the surface of the nanotube with a charge transfer from nanotube to HCN molecule. Due to the physisorption, NQR parameters of nanotube are also altered. In order to examine the deformation degree of the nanotube after HCN molecule adsorption, deformation energy is calculated, which indicates that no significant curvature in the geometry of the nanotubes is occurred when HCN adsorbs onto the surface of BeONT.

Keywords Adsorption · BeONT · HCN · Adsorption energy · NMR · AIM · NBO

✉ Mina Marvi
minamarvi@birjand.ac.ir

[1] Chemistry Department, University of Birjand, Birjand, Iran

Introduction

Hydrogen cyanide is colorless and extremely poisonous liquid. This compound and its derivatives are used for many chemical processes, including fumigation, the case hardening of iron and steel, electroplating, and the concentration of ores. It also is employed in the preparation of acrylonitrile, which is used in the production of acrylic fibers, synthetic rubber, and plastics. Hydrogen cyanide is highly toxic because it inhibits cellular oxidative processes. An adult human can withstand 50–60 parts of hydrogen cyanide per million parts of air for an hour without serious consequences, but exposure to concentrations of 200–500 parts per million of air for 30 min is usually fatal. Controlling the HCN concentration under the threshold limit value in the air requires a sensitive, reliable, and specific method for monitoring its content in work environments. Due to detect HCN concentration in the air, gas sensors have been considered promising alternatives for environmental measurements due to their low cost, high sensitivity, fast response and direct electronic interface [1, 2]. In recent years, nanotubes have attracted great interest in the sensor industry. Carbon nanotubes (CNTs) as chemical sensors [3–5] have generated strong interests in the research community since Kong et al. [3, 4] demonstrated that single-walled carbon nanotubes (SWCNT) can be used as miniature sensors to detect low concentrations of toxic gas molecules.

Valentini et al. [6] showed that CNTs could detect poison gas concentrations as small as 10 ppb. However, since the electronic properties of CNTs are mainly dependent on tabular chirality and diameter [7], separation of nanotubes with the desired electronic properties from other kinds is very difficult.

Recently, models of pristine single-walled beryllium oxide nanotubes are proposed. Due to the large ionicity of

Be–O bond, BeO compound often displays different properties from the counterpart of C, BN and SiC. BeO is an insulator with wide band gap (about 10 eV), high melting point, high thermal conductivity and large elastic constants [8]. In addition, compared with CNTs, BNNTs and SiCNTs, it is found that the BeONTs have a larger band gap which is less dependent on the chirality and the diameter of tubes [9, 10].

In this work, the adsorption energies, optimized parameters, the molecular orbital properties like HOMO, LUMO, chemical potential, hardness, their energy gap and AIM, NBO, NMR, NQR calculations and density of states (DOS) plots are used to gain insights into the influence of HCN adsorption on the electronic properties, geometrical structure of the BeONT, and how these effects could be used to design more sensitive gas sensing devices.

Computational methods

To study the adsorption behavior of HCN molecule, armchair (5,5) single-walled BeONT consisting of 35 pairs Be and O atoms has been chosen as model where open ends are saturated by hydrogen atoms. Geometry optimizations have been carried out by the DFT method by employing Becke, 3-parameter, Lee–Yang–Parr (B3LYP) functional [11, 12] with 6-31G* basis. Harmonic vibrational frequency calculations have been carried out to check whether the configurations are minima or not. The binding energy is corrected using the counterpoise technique proposed by Boys and Bernardi [13] and zero-point vibrational energy (ZPVE) correction. The adsorption energy (E_{ads}) is estimated using the following approximate expression:

$$E_{ads} = E_{HCN/BeONT} - (E_{BeONT} + E_{HCN}) \quad (1)$$

where $E_{HCN/BeONT}$ corresponds to the energy of the BeONT, in which the HCN molecule has been adsorbed on its wall, E_{BeONT} is the energy of the isolated nanotube and E_{HCN} is the energy of a single HCN molecule. It should be mentioned that the adsorption energy is the sum of interaction and deformation energy. The following equations are applied to calculate these contributions.

$$E_{ads} = E_{def} + E_{int} \quad (2)$$

$$E_{int} = E_{tube-gas} - \left(E_{tube\ incomplex} + E_{gas\ in\ complex}\right) \quad (3)$$

$$E_{def} = E_{def\ gas} + E_{def\ tube} \quad (4)$$

where $E_{tube\ in\ complex}/E_{gas\ in\ the\ complex}$ is the total energy of nanotube/gas and $E_{def\ tube}/E_{def\ gas}$ is the deformation energy of nanotube/gas in its optimized geometry.

The quantum molecular descriptors like energy gap, global hardness and chemical potential are used for explaining the chemical reactivity and stability of the different configurations. The energy gap is defined as $Eg = E_{LUMO} - E_{HOMO}$; E_{LUMO} is the energy of the lowest unoccupied molecular orbital and E_{HOMO} is the energy of the highest occupied molecular orbital. The chemical potential (μ) and global hardness (η) can be calculated as follows [14–16]:

$$\eta = \frac{E_{LUMO} - E_{HOMO}}{2} \quad (5)$$

$$\mu = \frac{E_{LUMO} + E_{HOMO}}{2} \quad (6)$$

The AIM 2000 program [17] is used in calculating the properties of the bond critical points; their electron densities and their Laplacians. The NBO [18] calculation is performed by using the NBO 3.1 program [19], as implemented in the Gaussian 03 package [20].

The Wiberg bond index (WBI) which comes from the manipulation of the density matrix in the orthogonal natural atomic orbital based on the NBO analysis [21, 22] is also considered. WBI demonstrates the strength of the covalent character (the larger WBI implies to stronger covalent character) and closely relates to the bond order. WBI expressed by the following mathematical definition:

$$WBI = \sum\nolimits_k P_{jk}^2 = 2P_{jj} - P_{jj}^2 \quad (7)$$

where P_{jk} and P_{jj} denote the density matrix elements and charge density in the atomic orbital, respectively.

Molecular electrostatic potential (MEP) surfaces for all of the configurations under study are generated using the electron density at the B3LYP/6-31G* level. The work function is determined as the difference between the vacuum level and the Fermi level, which herein, the energy of vacuum level has been assumed to be zero. The canonical assumption for Fermi level is that in a molecule (at $T = 0$ K) it lies approximately in the middle of the Eg. The work function represents the minimum energy required to remove an electron from the Fermi level to the vacuum level. Furthermore, in order to investigate the effects of the HCN adsorption on the electronic properties of the nanotube, the density of state (DOS) analysis is performed.

Experimentally, quadrupole coupling constants (C_Q) and asymmetry parameters (η_Q) are measured by nuclear quadrupolar resonance (NQR). C_Q is the interaction energy of the nuclear electric quadrupole moment (e) with the EFG tensors at the sites of quadrupole nuclei, but the asymmetry parameter (η_Q) is a quantity of the EFG tensors that describes the deviation from tubular symmetry at the sites of quadrupole nuclei. Quantum chemical calculations yield principal components of the EFG tensor, q_{ii}, in atomic unit

$$1\,au = 9.717365 \times 10^{21}\,V\,m^{-2}$$

The calculated EFG tensor eigenvalues in the principal axis system (PAS) with order $|q_{zz}| > |q_{yy}| > |q_{xx}|$ are

converted to measurable NQR parameters, C_Q and η_Q, using Eqs. (8) and (9). Standard Q values [(^{9}Be) = 52.88 and (^{17}O) = 25.58 mb] reported by Pyykkö [23] are used in Eq. (8) [23, 24].

$$C_Q(\mathrm{MHz}) = e^2 Q q_{zz} \mathrm{h}^{-1} \tag{8}$$

$$\eta_{\mathrm{Q}} = \left|\left(q_{\mathrm{xx}} - q_{\mathrm{yy}}\right)/q_{\mathrm{zz}}\right| \quad 0\langle\eta_{\mathrm{Q}}\langle 1 \tag{9}$$

The global interaction between the HCN molecule and BeONT can be showed by the parameter ΔN which determines the fractional number of electrons transferred from a system A to system B and can be calculated as follows:

$$\Delta N = (\mu_{\mathrm{B}} - \mu_{\mathrm{A}})/(\eta_{\mathrm{A}} + \eta_{\mathrm{B}}) \tag{10}$$

which yields stabilization energy (ΔE_{SE}) to be as:

$$\Delta E_{\mathrm{SE(AB)}} = \Delta E_{\mathrm{A(B)}} + \Delta E_{\mathrm{B(A)}} = -(\mu_{\mathrm{B}} - \mu_{\mathrm{A}})^2/2(\eta_{\mathrm{A}} + \eta_{\mathrm{B}}) \tag{11}$$

From Eq. (11) it is obvious that in the process of spontaneous flow of the electrons from one species to another, ΔE_{SE} is negative. Therefore, the interaction between two species is favorable. However, spontaneous flow of the electrons from B to A cannot be predicted from the negative value of the ΔE_{SE} alone. This formation can obtain from ΔN, the positive value of ΔN, indicates that electron flow is spontaneous from B to A; otherwise, it is in the reverse direction. Also, information regarding the direction of the electron transfer can be extracted from components of the ΔE_{SE} ($\Delta E_{\mathrm{B(A)}}$ and $\Delta E_{\mathrm{A(B))}}$ and can be denoted as:

$$\Delta E_{\mathrm{B(A)}} = \Delta N(-\mu_B + \frac{1}{2}\eta_B \Delta N) \tag{12}$$

$$\Delta E_{\mathrm{A(B)}} = \Delta N(-\mu_{\mathrm{A}} + \frac{1}{2}\eta_{\mathrm{A}} \Delta N) \tag{13}$$

The positive $\Delta E_{\mathrm{B\ (A)}}$ value demonstrates that B is a donor and A is the acceptor [25]. Similar argument indicates that $\Delta E_{\mathrm{A\ (B)}}$ will be negative when A in the donor and B is the acceptor.

The chemical shielding tensors (CS) at the sites of Be and O nuclei are calculated using the gauge-independent atomic orbital (GIAO) method [26]. The quantum chemical calculations yield chemical shielding tensors in the principal axis system (PAS) with the order of $\sigma_{33} > \sigma_{22} > \sigma_{11}$; therefore, Eqs. (14) and (15) are used to convert the calculated chemical shielding tensors to the absolute isotropic (σ_{iso}) and anisotropic ($\Delta\sigma$) chemical shielding parameters:

$$\sigma_{\mathrm{iso}} = (\sigma_{33} + \sigma_{22} + \sigma_{11})/3 \tag{14}$$

$$\Delta\sigma = \sigma_{33} - (\sigma_{11} + \sigma_{22})/2 \tag{15}$$

Results and discussion

Molecular geometry and binding energies

Full structural optimization of pristine BeONT and several potential configurations (HCN is placed at the different position on the nanotube surface) is carried out to explore the adsorption energy of the HCN molecule on the exterior and interior surfaces of the BeONT. Table 1 illustrates the geometrical parameters and the interaction (E_{int}), deformation (E_{def}) and adsorption (E_{ads}) energies for the studied complexes. The value of the obtained adsorption energies varies from 18.09 to −14.02 kJ/mol. These results indicate that the HCN molecule can be physically adsorbed on the surface of the BeONT and in the most cases the adsorption process on the exterior surface is exothermic, while HCN adsorption on the interior surface is endothermic.

In order to identify the most stable configuration, we investigate several potential configurations, including the HCN molecule is initially placed above beryllium and oxygen atoms which the HCN molecule approached to the nanotube wall from N-down, H-down, and several configurations with HCN molecule orientations parallel to the nanotube surface, above of the hexagonal ring. The notation N-down and H-down denotes an HCN perpendicular to the surface via N and H atoms, and two cases for its adsorption on the inside of the nanotube (HCN perpendicular and parallel to the z axis of the nanotube) have been considered. After structural optimizations, re-orientation of the molecule has been predicted in some configurations, and finally, stable configurations are obtained. The initial and final optimized geometry of the HCN/BeONT complexes is depicted in Fig. 1.

Inspection of the results shows that the most stable configuration (N-side) is configuration 1 which in this configuration, the N atom of the HCN molecule prefers to attach to Be atom of the nanotube by a distance of 1.852 Å. The adsorbed HCN causes the Be1–O2 bond length increases from 1.551 of the free nanotube to 1.601 Å in the HCN adsorbed form because the absorption of HCN on the BeONT causes the SP^2 hybridization of the Be atom in the Be1–O2 bond change to the SP^3 hybridization and hence the Be1–O2 bond length increases. As known, the isolated HCN molecule is planar molecule with the H–C–N angle of 180°. When the HCN molecule adsorbs on the exterior surface of the nanotube, the HCN angle does not considerably change. Also, the C≡N bond length in the configuration 1 is about 1.150 Å, which slightly is shorter than that in the free molecule. Here, it should be stated that the stretching mode of C≡N bond in the configuration 1 (2263.16 cm^{-1}) occurs at larger frequencies compared to that of the free molecule (2214.86 cm^{-1}), indicating that

Table 1 The geometrical parameters (bond lengths (R), in Å), adsorption (E_{ad}), interaction (E_{int}) and deformation (E_{def}) energies (kj mol^{-1}) calculated at the B3LYP/6-31G* level

			$R_{C\equiv N}$	R_{C-H}	E_{ads}	E_{int}	E_{def}
Configuration 1	Be1–O6 = 1.6307 Be1–O2 = 1.6007	Be1···N = 1.8517	1.15009	1.07165	−14.02	−44.84	30.81
Configuration 2	Be3–O2 = 1.5947 Be3–O4 = 1.5968	Be3···N = 1.99273	1.15027	1.07207	−13.14	−42.35	29.21
Configuration 3	Be17–O7 = 1.5967 Be17–O18 = 1.5858	Be17···N = 1.9434	1.15055	1.07213	−11.82	−39.17	27.34
Configuration 4	Be17–O7 = 1.5967 Be17–O18 = 1.5858	Be17···N = 1.9434	1.15055	1.07212	−11.82	−39.17	27.34
Configuration 5	Be17–O7 = 1.5968 Be17–O18 = 1.5858	Be17···N = 1.9433	1.15055	1.07212	−11.82	−39.16	27.34
Configuration 6	Be3–O4 = 1.5968 Be3–O2 = 1.5946	Be3···N = 1.9272	1.15027	1.07207	−13.12	−42.33	29.20
Configuration 7	Be17–O7 = 1.5967 Be17–O18 = 1.5858	Be17···N = 1.9434	1.15055	1.07212	−11.83	−39.17	27.34
Configuration 8	O2–Be1 = 1.5627 O2–Be15 = 1.5472	O2···H = 2.2977	1.15751	1.07511	−0.23	−1.81	1.58
Configuration 9	Be17–O7 = 1.5967 Be17–O18 = 1.5858	Be17···N = 1.9434	1.15055	1.07212	−11.83	−39.17	27.35
Configuration 10	O2–Be1 = 1.5627 O2–Be15 = 1.5473	O2···H = 2.2977	1.15751	1.07511	−0.22	−1.79	1.56
Configuration 11	O7–Be17 = 1.5609 O7–Be8 = 1.5604	O7···H = 2.2678	1.15751	1.0756	1.08	0.08	1.00
Configuration 12	Be3–O4 = 1.5968 Be3–O2 = 1.5938	Be3···N = 1.9273	1.15027	1.07207	−13.14	−42.34	29.21
Configuration 13	Be3–O7 = 1.5562 Be3–O4 = 1.5445	O7···H = 2.2167	1.15631	1.07623	18.09	11.96	6.13
Configuration 14	Be3–O7 = 1.554	O7···C = 3.5313	1.15706	1.07152	12.68	8.92	3.76

the length of C≡N bond should be decreased upon the HCN adsorption process. The calculated E_{ad} value is about −14.02 kJ/mol for the most stable configuration that exhibiting a physisorption characteristic. Also, the negative E_{ad} value confirms that this process energetically is favorable and exothermic. It can be seen from Table 1, the nanotube···molecule distance in the configuration 1 is shorter than that the other configurations. This can be attributed to stronger interaction in this configuration.

The most stable configuration for HCN adsorption in H-down orientation is configuration 8. In this configuration, HCN preferentially interacts via its H atom with O atom in the nanotube (see Fig. 1). The calculations show that the adsorption energy for this configuration is about −0.23 kJ/mol with equilibrium distance 2.30 Å. Analysis of the structural parameters indicates that the C≡N and Be–O bonds length are remained nearly constant. These results confirm that the interaction in this configuration is from type of weak interactions. From the adsorption energies presented in Table 1, it can be seen that the adsorption energies depend on the locations and orientations of HCN molecule. On the other hand, calculated adsorption energy for the configurations which in those the HCN adsorbed on the BeONT via its N atom is more notable than that adsorption via its H atom. Therefore, it is worth mentioning that HCN interaction via N atom is stronger than the other configurations.

In the configuration in which the HCN molecule adsorbs from the N-side, the computed C≡N equilibrium bond distance of absorbed molecule is shorter than its corresponding bond length in the isolated HCN molecule, 1.157 Å. This fact indicates the CN bond in adsorbed models becomes strong by interacting with the BeONT. Our theoretical results show that the adsorption energy of the HCN molecule on the internal surface is positive which indicate the addition reaction is endothermic and the formed complexes are unstable.

The obtained deformation energy values for the investigated configurations vary from 1 to 30.81 kJ/mol, which indicates that no significant curvature in the geometry of

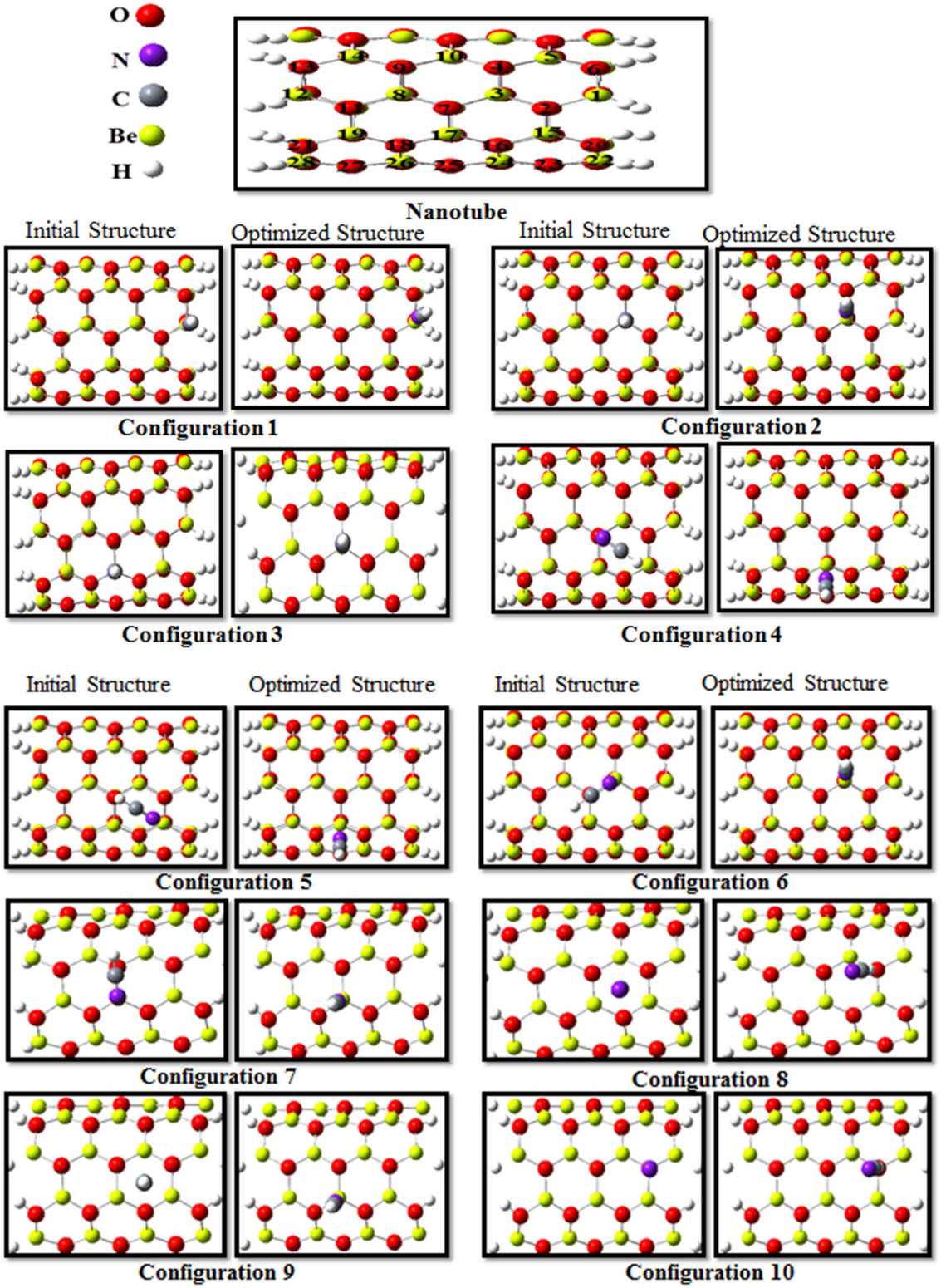

Fig. 1 Initial and optimized structures for different configurations

these nanotubes is occurred when HCN adsorbs onto the surface of BeONT. On the other hand, the contribution of the interaction energies for the studied configurations (see Table 1) confirms that HCN molecule could be physisorbed onto the BeONT surface. Also, structural parameters and deformation energy indicate that the

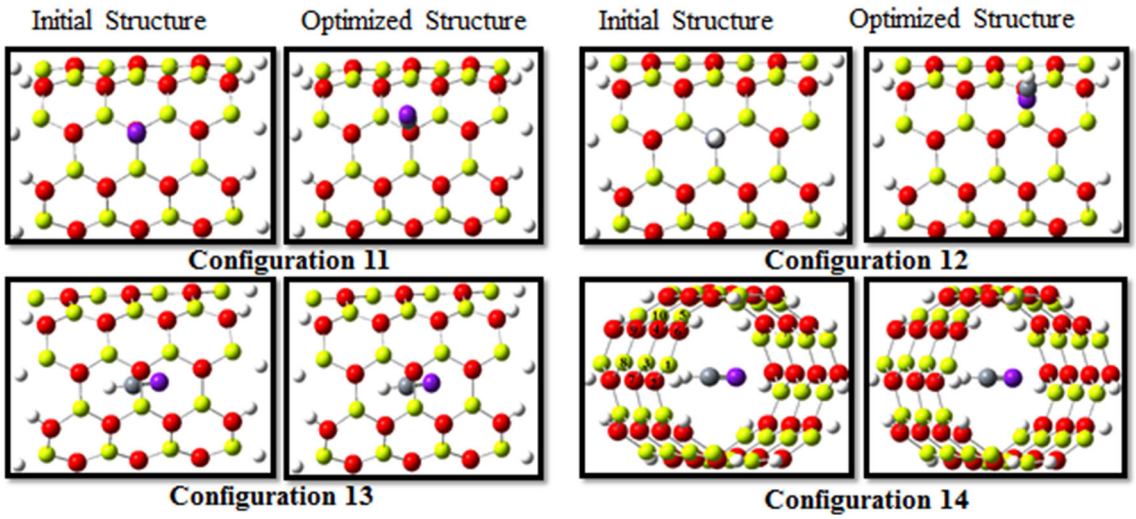

Fig. 1 continued

deformation degree in configurations in which HCN adsorbs on the BeONT via the N atom is more than the other configurations.

In order to determine the direction of electron transfer when two species (nanotube and HCN molecule) form complex, we calculate ΔN, $\Delta E_{B\ (A)}$ and $\Delta E_{A\ (B)}$. Our theoretical results indicate that ΔN and $\Delta E_{B\ (A)}$ (B = nanotube and A = HCN) are positive and $\Delta E_{A\ (B)}$ is negative ($\Delta N = 0.\ 375$, $\Delta E_{B\ (A)} = 1.782$ and $\Delta E_{A\ (B)} = -1.366$). Therefore, electron flow is spontaneous from nanotube to HCN molecule.

Investigation of the theoretical results reveals that there is a good correlation between nanotube···HCN bond length versus the adsorption energy with a correlation coefficient about 0.99 and linear regression is given by equation presented below:

$$Y = 34.918\,x - 79.783 \tag{16}$$

where Y corresponds to adsorption energy and x corresponds to the nanotube···HCN bond length. These imply that the nanotube···HCN bond length can be very useful to estimate the adsorption energy.

Aim analysis

In order to obtain the deeper insight into the nature and strength of the nanotube-molecule interaction in considered systems, the analysis of electron density has been carried out. The ρ_{BCP}, $\nabla^2\rho_{BCP}$ and the G_{BCP}, V_{BCP} and H_{BCP} energy component values for all of the models examined in this work are shown in Table 2.

Analysis of topological parameters for the studied configurations shown in Table 2 reveals that the BCPs (bond critical point) corresponding to the $Y\ldots X$ (Y = Be or O of the nanotube and X = H or N atom of the HCN) contact have positive H_{BCP} and $\nabla^2\rho_{BCP}$ values. Their values are in the range of 0.0408–0.2633 au for $\nabla^2\rho_{BCP}$ which indicates that the interaction in the analyzed systems may be classified as electrostatic interactions.

Inspection of the topological parameters confirms that in the most stable configuration, in comparison with pristine BeONT, the electron density at the BCP of Be1–O2 bond decreases. This result is supported by an increase in the Be1-O2 bond length. Also, the C≡N electron density is enhanced from 0.466 to 0.468 a.u after the adsorption process which is consistent with the shortening of the C≡N bond length. In addition, in the most stable configuration, the electron density at the BCP of the nanotube···HCN contact is higher than that of the other configurations which can be attributed to stronger interaction in this configuration. Therefore, analysis of the electron density for the studied complexes indicates that the electron density at the BCP of nanotube···HCN contact becomes more as the interaction energy becomes larger. Furthermore, it can be seen from Table 2, the increase in ρ results in the decrease in the distance between HCN and nanotube. The electron densities of the nanotube···N_{HCN} contact is more than the corresponding value for nanotube···H_{HCN} contact, showing the more effective interaction in the former case. In addition, in the configurations 10,12, because of the weak interaction between HCN molecule and nanotubes, the values of $\rho(r)$ at BCPs of Be–O bonds in the complexes around the adsorbing area almost did not undergo noticeable changes in comparison with the pristine nanotube (see Table 2).

The nature of the binding between BeONT and HCN molecule has been analyzed from the calculated total electron density maps. The isosurface maps for the HCN adsorption are

Table 2 Topological properties (in au) of different configurations calculated at the B3LYP/6-31G* level

	Be–O		C≡N		C–H		Nanotube···HCN	
	ρ	$\nabla^2\rho$	ρ	$\nabla^2\rho$	ρ	$\nabla^2\rho$	ρ	$\nabla^2\rho$
Configuration 1	Be1–O6 = 0.0717	0.536242	0.468203	0.518183			Be1···N = 0.0401	0.26329
	Be1–O2 = 0.0805	0.589539						
Configuration 2	Be3–O2 = 0.0830	0.592134	0.469021	0.493705	0.281245	−1.17123	Be3···N = 0.0334	0.200164
	Be3–O4 = 0.0822	0.58862						
Configuration 3	Be17–O7 = 0.0826	0.589445	0.46896	0.487752	0.281205	−1.17063	Be17···N = 0.0320	0.1901
	Be17–O18 = 0.0850	0.614523						
Configuration 4	Be17–O7 = 0.0826	0.589444	0.46896	0.487752	0.281206	−1.17064	Be17···N = 0.0320	0.190099
	Be17–O18 = 0.0850	0.614525						
Configuration 5	Be17–O7 = 0.0826	0.589298	0.468959	0.487768	0.281207	−1.17065	BE17···N = 0.0320	0.190177
	Be17–O18 = 0.0850	0.614579						
Configuration 6	Be3–O4 = 0.0822	0.588476	0.469017	0.493839	0.281246	−1.17122	Be3···N = 0.0334	0.20019
	Be3–O2 = 0.0830	0.592293						
Configuration 7	Be17–O7 = 0.0826	0.589444	0.46896	0.487742	0.281207	−1.17064	Be17···N = 0.0320	0.190096
	Be17–O18 = 0.0850	0.614529						
Configuration 8	O2–Be1 = 0.0895	0.685475	0.467225	0.449542	0.279318	−1.14591	O2···H = 0.0137	0.040853
	O2–Be15 = 0.0951	0.715279						
Configuration 9	Be17–O7 = 0.0826	0.589429	0.46896	0.487746	0.281207	−1.17064	Be17···N = 0.0320	0.190097
	Be17–O18 = 0.0850	0.614518						
Configuration 10	O2–Be1 = 0.0896	0.685492	0.467224	0.449568	0.279319	−1.14591	O2···H = 0.0137	0.040862
	O2–Be15 = 0.0950	0.715132						
Configuration 11	O7–Be17 = 0.0912	0.680497	0.467264	0.446813	0.278938	−1.14311	O7···H = 0.0147	0.042439
	O7–Be8 = 0.0919	0.679065						
Configuration 12	Be3–O4 = 0.0822	0.588581	0.469022	0.493709			Be3···N = 0.0334	0.200161
	Be3–O2 = 0.0834	0.594612						
Configuration 13	Be17–O7 = 0.0924	0.69351	0.468039	0.42512	0.27910	−1.15700	O7···H = 0.0174	0.050907
Configuration 14	Be3–O7 = 0.09335	0.69571	0.468039	0.42512	0.28216	−1.16435	O7···C = 0.00379	0.013711

shown in Fig. 2. In configuration 1, the HCN molecule remains far from the cage having almost no effect on the electronic charge distribution of atoms of the nanotube. Therefore, no significant charge transfer is occurred which is in agreement with low adsorption energies of this complex.

We can find (see Fig. 3) a weak overlap of the electron densities between HCN and BeONT, which means that HCN molecule is physically adsorbed on the nanotube surface.

Natural bond orbital analyses (NBO)

The NBO analysis is employed to study the intermolecular orbital interaction in the complexes. The results of our NBO analysis for studied configurations are provided in Table 3.

The theoretical results indicate that due to the positive charge accumulated on the Be atom and the negative charge on the N atom of the HCN, we expect an attractive interaction between the nanotube and HCN molecule. A comparison between the electrical charge of the Be of the nanotube before (0.183 e) and after (0.293 e) adsorption indicates that the nanotube acts as an electron donor.

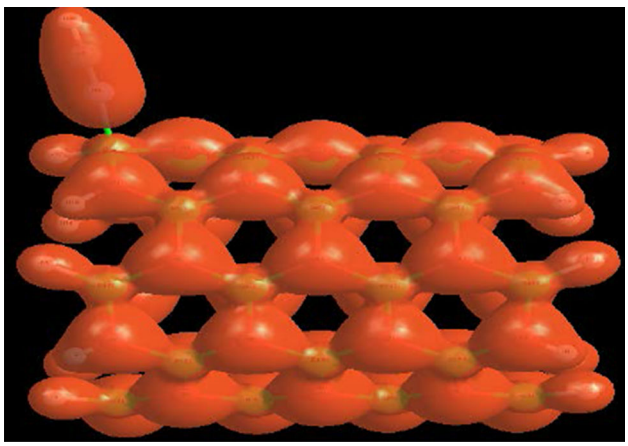

Fig. 2 Isosurfaces of the total electron density for the HCN adsorption on BeONT in configuration 1

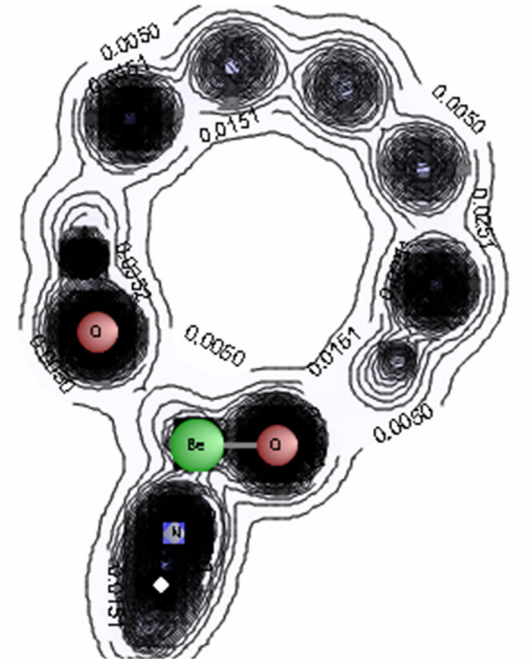

Fig. 3 The contour map of configuration 1 obtained from the DFT calculation

According to NBO analysis, the most important donor–acceptor interaction in the most stable configuration is $\sigma_{Be-N} \rightarrow \sigma^*_{C-N}$ interaction. Therefore, σ_{Be-N} participates as donor and σ^*_{C-N} behaves as an acceptor in strong intermolecular charge transfer interactions with the energy value of 7.90 kcal/mol. Thus, the HCN molecule acts as an electron acceptor. Also, our theoretical results indicate that charge transfer occurs from σ_{Be-N} to σ^*CH. It is noteworthy that this is the primary effect which causes elongation of the C–H bond. The elongation induces structural reorganization of the HCN molecule including contraction of the CN bond.

On the other hand, the most important donor–acceptor interaction in the configuration 14 is $LP_{O7} \rightarrow \sigma^*_{C-H}$ interaction. Therefore, LP_{O7} (lone pair) plays the role of a donor, while σ^*_{C-H} behaves as an acceptor in the intermolecular charge transfer interactions with the energy value of 3.6 kcal/mol. Also, when HCN adsorbs on the exterior and interior surface, HCN acts as an electron acceptor and BeONT acts as an electron donor.

The influence of adsorption process on the occupation numbers of σ^*_{C-N} has also investigated. In the most stable configuration, HCN adsorption on the nanotube surface results in an increase of the occupation number of the σ^*_{C-N}. These results confirm that the lost charge from the nanotube is shifted to σ^*_{C-N} upon the adsorption process.

Analysis of NBO indicates that by adsorption of the HCN molecule on the nanotube surface in the most stable configuration, the p' character of Be1 atom in the Be1–O2 bond of the nanotube is changed from 67.91 to 73.47 %, indicating the elongation of Be1–O2 bond after adsorption of the HCN molecule, which is in accordance with previous results in this work. Also, the influence of HCN-nanotube interaction on the bond order has investigated in this study. The smaller WBI implies to weaker covalent character. The analysis of WBI illustrates that in the configuration 1, the adsorption of HCN on the exterior surface of the BeONT leads to decrease in the WBI of Be1-O2 from 0.1508 to 0.1229. These results are in agreement with obtained structural parameters for this configuration.

It can be seen from Table 3, $E^{(2)}$ value for the different configurations varies from 0.28 to 9.29 kcal/mol. It is well known that the larger is the $E^{(2)}$, the stronger is the interaction between HCN and nanotube and the greater the tendency that nanotube provide electron to HCN molecule, means more charge transferred. Therefore, there is stronger interaction in the configurations which in those the HCN adsorbs on the BeONT via the N atom in comparison with the configurations which the HCN interacts with the BeONT via its H atom, because of more total charge transfer energy associated with the intermolecular interaction.

Thermodynamic parameters

The calculated thermodynamic properties of the investigated systems are shown in Table 4. The complexes with lower relative standard Gibbs energy of formation are relatively more stable, whereas those with the higher relatively standard energy of formation are more unstable. The negative standard enthalpy change demonstrates that the formation of complexes is enthalpically favored. The values of the $T\Delta S^0_{298}$ imply the large entropy changes during the formation of complexes. In the investigated complexes, the high negative values of the $T\Delta S^0_{298}$ determine the positive values of ΔG^0_{298}. Thus, the formation of complexes is thermodynamically disfavored $(\Delta G^0_{298} \rangle 0)$.

HOMO and LUMO analysis

LUMO and HOMO profiles of the HCN molecule, pristine BeONT and configurations 1 and 8 have been shown in Fig. 4. It can be seen that the HOMO of HCN molecule is positioned on whole of the molecule and LUMO is located on the N atom and C-H bond. Molecular orbital plots for HOMO and LUMO levels of pristine BeONT show the HOMO positions at the two ends of the nanotube, which suggests that the ends of the nanotube are more reactive compared to the side wall.

The molecular orbital plots of configuration 8 indicate that after HCN adsorption, the LUMO is localized on the

Table 3 $E^{(2)}$ (Kcal/mol) corresponds to charge transfer, WBI and the G_{BCP}, V_{BCP} and H_{BCP} energy component values computed at the B3LYP/6-31G* level of theory

	Donor → acceptor	$E^{(2)}$		WBI			G	V	H
Configurations 1	LPO6 → σ*Be1–N	7.83	σ*C–N = 0.01172	Be1–O6 = 0.1229	C–H = 0.9228	Be1···N	0.05739	−0.0489	0.00842
	Be1–N → σ*C–N	7.9	LPO6 = 1.90441	Be1–O2 = 0.1253	C≡N = 2.8912				
Configuration 2	σBe3–N → σ*C–H	9.25	σ*C–H = 0.00716	Be3–O2 = 0.1380	C–H = 0.9222	Be3···N	0.04329	−0.0365	0.00674
	σBe3–N → σ*C–N	7.42		Be3–O4 = 0.1393	C≡N = 2.9093				
Configuration 3	σBe17–N → σ*C–N	7.23	σ*C–H = 0.00773	Be17–O7 = 0.1417	C–H = 0.9221	Be17···N	0.04095	−0.0343	0.00657
	σBe17–N → σ*C–H	9.29	C–N = 0.01080	Be17–O18 = 0.1408	C≡N = 2.9107				
	LPO18 → σ*Be–N	7.5	LPO18 = 1.82168						
Configuration 4	LPO18 → σ*Be17–N	7.5	LPO7 = 1.82245	Be17–O7 = 0.1417	C–H = 0.9221	Be17···N	0.04095	−0.0343	0.00657
	LPO16 → σ*Be17–N	7.5	LPO16 = 1.82168	Be17–O18 = 0.1408	C≡N = 2.9107				
	LPO7 → σ*Be17–N	7.29	LPO18 = 1.82168						
Configuration 5	LPO16 → σ*Be7–N	7.51	σ*C–N = 0.01081	Be17–O7 = 0.1417	C–H = 0.9221	Be17···N	0.04095	−0.0343	0.00657
	LPO18 → σ*Be17–N	7.5	LPO16 = 1.82172	Be17–O18 = 0.1408	C≡N = 2.9107				
	σBe17–N → σ*C–N	7.23	LPO18 = 1.82170						
Configuration 6	LPO7 → σ*Be3–N	7.23	σ*C–N = 0.01101	Be3–O4 = 0.1393	C–H = 0.9222	Be3···N	0.0433	−0.0365	0.00674
	LPO2 → σ*Be3–N	7.35	LPO = 1.81768	Be3–O2 = 0.1380	C≡N = 2.9093				
	σBe3–N → σ*C–N	7.42	LPO = 1.81853						
Configuration 7	LPO16 → σ*Be17–N	7.5	C–N = 0.01080	Be17–O7 = 0.1417	C–H = 0.9221	Be17···N	0.04095	−0.0343	0.00657
	LPO18 → σ*Be17–N	7.5	LPO16 = 1.82168	Be17–O18 = 0.1408	C≡N = 2.9107				
	σBe17–N→σ*C–N	7.23	LPO18 = 1.82168						
Configuration 8	LPO2 → σ*C–H	3.92	σ*C–H = 0.02445	O2–Be1 = 0.1494	C–H = 0.9090	O2···H	0.00906	−0.0079	0.00115
	Be3–O2 → σ*C–H	0.28	LPO2 = 1.81544	O2–Be15 = 0.1874	C≡N = 2.9877				
	Be15–O2 → σ*C–H	0.67							
Configuration 9	LPO16 → σ*Be17–N	7.5	σ*C–H = 0.00773	Be17–O7 = 0.3727	C–H = 0.9197	Be17···N	0.04095	−0.0343	0.00657
	LPO18 → σ*Be17–N	7.5	σ*C–N = 0.01080	Be17–O18 = 0.3755	C≡N = 2.9020				
	Be17–N → σ*C–H	9.29	LPO16 = 1.82168						
	Be17–N → σ*C–N	7.23	LPO18 = 1.82168						
Configuration 10	LPO2 → σ*C–H	3.92	σ*C–H = 0.02445	O2–Be1 = 0.4069	C–H = 0.9133	O2···H	0.00906	−0.0079	0.00115
	σBe15–O2 → σ*C–H	0.67	LPO2 = 1.81544	O2–Be15 = 0.4283	C≡N = 2.9868				
Configuration 11	LPO7 → σ*C–H	4.32	σ*C–H = 0.02578	O7–Be17 = 0.4163	C–H = 0.9128	O17···H	0.0096	−0.0086	0.001
	σBe17–O7 → σ*C–H	0.62	LPO7 = 1.81507	O7–Be8 = 0.4084	C≡N = 2.9875				
Configuration 12	LPO2 → σ*Be3–N	7.34	LPO2 = 1.82439	Be3–O4 = 0.4809	C–H = 0.9198	Be3···N	0.04329	−0.0365	0.00674
	LPO4 → σ*Be3–N	7.13	LPO4 = 1.81762	Be3–O2 = 0.5071	C≡N = 2.9006				
	σBe3–N → σ*C–H	9.25	σ*C–H = 0.00764						
Configuration 13	LPO27 → σ*C–H	1.92	σ*C–H = 0.01645	Be3–O7 = 0.1745	C–H = 0.9118	O7···C	0.00255	−0.0017	0.00088
					C≡N = 2.960				
Configuration 14	LPO7 → σ*C–H	3.60	σ*C–H = 0.03326	Be7–O17 = 0.4058	C–H = 1.397	O7···H	0.01184	–0.0109	0.00088
					C≡N = 1.496				

Table 4 Changes in thermodynamic functions (kJ mol^{-1}) upon complex formation, energy of the highest occupied molecular orbital (E_{HOMO}), energy of the lowest unoccupied molecular orbital (E_{LUMO}), the molecular orbital energy gap, Eg, Chemical hardness (η) and chemical potential (μ) and work function (Φ) in terms of ev

	E_{HOMO}	E_{LUMO}	Eg	μ	η	Φ	ΔG	ΔH	$T\Delta S$
BeONT	−7.7452	−0.36122	7.38398	−4.05321	3.69199	4.05321	–	–	–
Configuration 1	−6.97653	−1.10242	5.87411	−4.03947	2.93705	4.03947	11.40444	−28.3159	−39.7204
Configuration 2	−7.45008	−1.19626	6.25382	−4.32317	3.12691	4.32317	10.80972	−26.9876	−37.7974
Configuration 3	−7.55453	−1.2104	6.34412	−4.38246	3.17206	4.38246	13.53966	−26.2148	−39.7544
Configuration 4	−7.55453	−1.2104	6.34412	−4.38246	3.17206	4.38246	13.53966	−26.2148	−39.7544
Configuration 5	−7.55453	−1.21067	6.3438	−4.3826	3.171929	4.3826	13.54228	−26.2174	−39.7597
Configuration 6	−7.44845	−1.19626	6.25219	−4.32235	3.12609	4.32235	10.83592	−26.9798	−37.8157
Configuration 7	−7.55453	−1.2104	6.34412	−4.38246	3.17206	4.38246	13.53966	−26.2148	−39.7544
Configuration 8	−7.81211	−0.49966	7.31244	−4.15589	3.65622	4.15589	22.82722	−2.66444	−25.4917
Configuration 9	−7.55453	−1.2104	6.34412	−4.38246	3.17206	4.38246	13.53704	−26.2148	−39.7518
Configuration 10	−7.81184	−0.49966	7.31217	−4.15575	3.65608	4.15575	22.83246	−2.66444	−25.4969
Configuration 11	−7.83986	−0.54454	7.29531	−4.1922	3.64765	4.19220	26.26454	−2.0933	−28.3578
Configuration 12	−7.44981	−1.19626	6.25355	−4.32303	3.12677	4.32303	10.81758	−26.9903	−37.8078
Configuration 13	−7.6565	−1.2498	6.4067	−4.4531	3.2033	4.45310	33.2911	−6.5419	−39.8330
Configuration 14	−7.6146	−1.2716	6.3430	−4.4431	3.1715	4.44310	32.5523	−10.6184	−43.1708

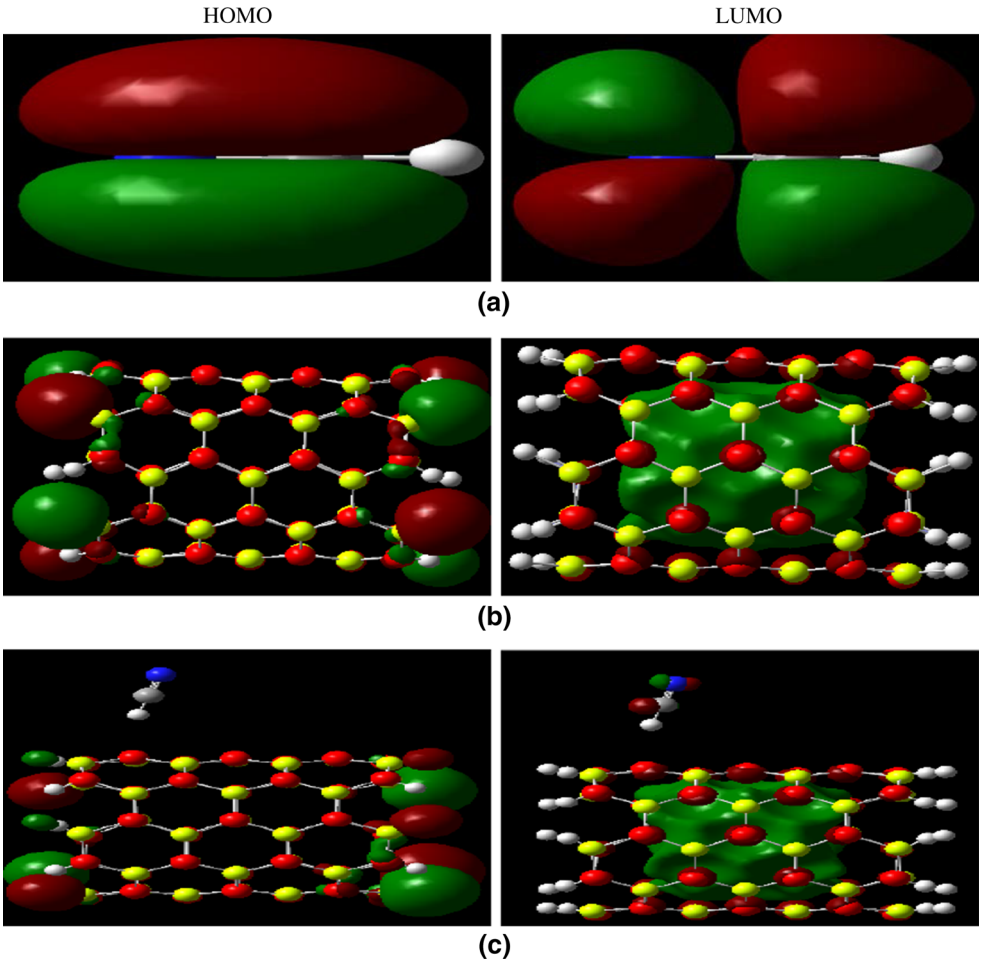

Fig. 4 Orbital depiction of HOMO and LUMO in **a** HCN molecule **b** BeONT **c** Configuration 8

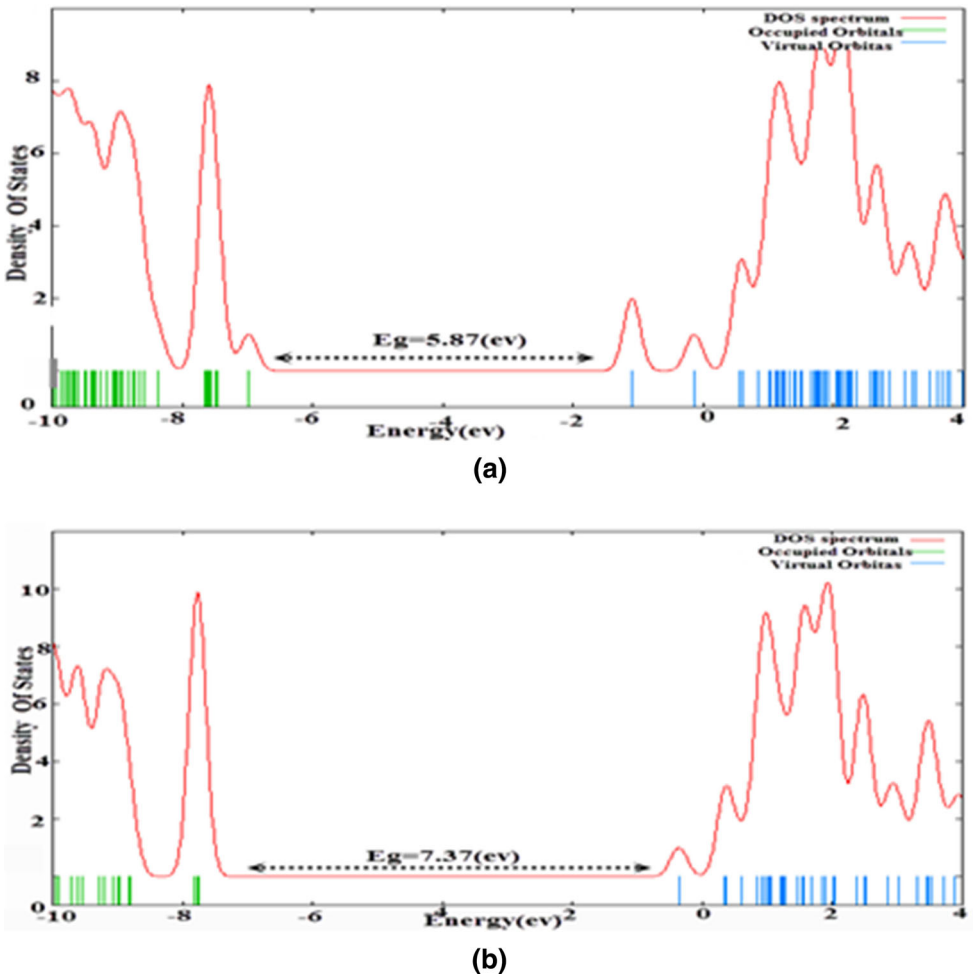

Fig. 5 The DOS of **a** the configuration 1, **b** BeONT

HCN and inside of the nanotube and the HOMO is placed at the two ends of the nanotube, indicating that electrons transfer from BeONT to HCN molecule.

It can be seen from Table 4 that HCN adsorption on the nanotube surface leads to decrease in the Eg and hardness, while the softness will be increased (see Table 4). Our computations also demonstrate that a charge transfer to take place between HCN and the outer surface of the nanotube, which shows that the stability between HCN and nanotube is lowered and their reactivity increased. Thus, when HCN approaches to the nanotube, electrons are transferred from the higher chemical potential to the lower chemical potential, until the electronic chemical potentials become identical. Hence, electrons will flow from a definite occupied orbital in BeONT and will go into a definite empty orbital in a single HCN. In addition, the electric conductivity of the BeONT will considerably change in the presence of HCN, which can be explained according to the following equation

$$\alpha \exp(-\mathrm{Eg}/2\mathrm{KT}) \tag{17}$$

where σ is the electrical conductivity and K is the Boltzmann's constant. According to this equation, smaller Eg values lead to the higher conductance at a given temperature.

We find that adsorption of HCN on the nanotube surface leads to reduce E_{LUMO} and increase E_{HOMO} for studied complexes. Inspection of the theoretical results indicates that the value of Eg in configuration 1 is lower than the other configurations which confirm its more reactivity in comparison with the other configurations. Therefore, it is energetically favorable to add electrons to a high-lying LUMO and to extract electrons from a low-lying HOMO. The maximum and minimum values of Eg correspond to the configurations 8 and 1, respectively (see Table 4).

In order to investigate the influence of HCN adsorption on the electronic properties of the nanotube, total electronic densities of states (DOSs) for all of studied systems have been calculated. Comparison of the DOS for configuration 1 with that of pristine type shows that after HCN adsorption, peaks appeared near the valence and conduction level of the

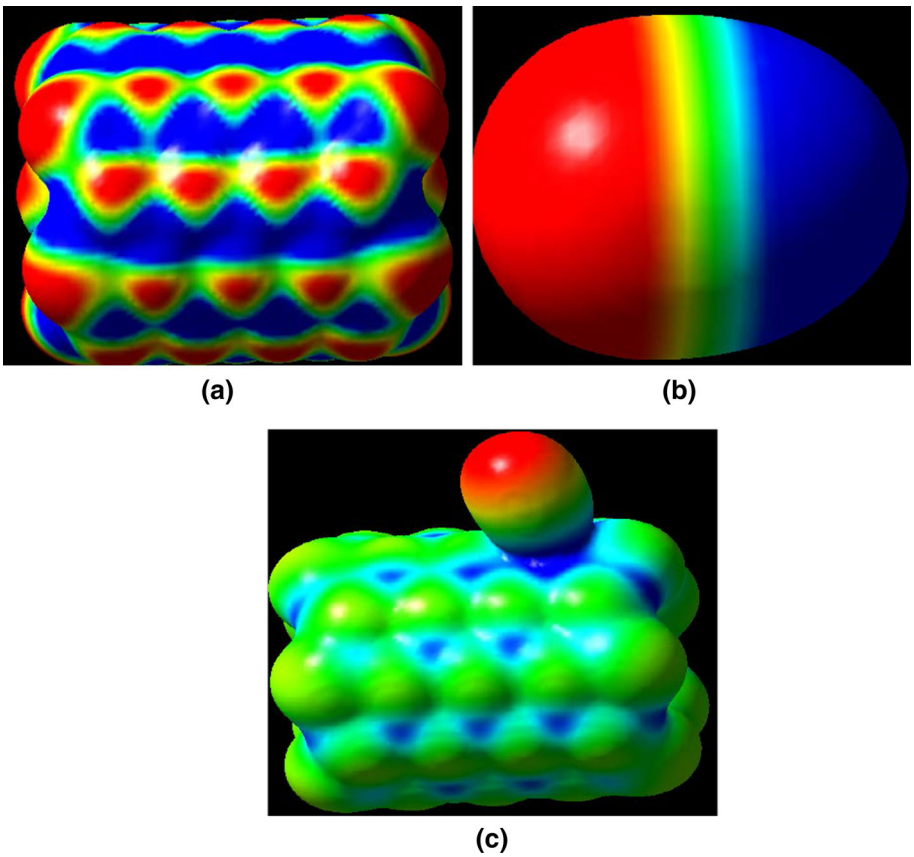

Fig. 6 Molecular electrostatic plots for **a** BeONT, **b** HCN molecule and **c** Configuration 8

nanotube (see Fig. 5), reducing the Eg of nanotube from 7.38 in free form to 5.87 eV in adsorbed form. Therefore, the DOS of nanotube shows the changes due to HCN adsorption in the gap regions of the DOS plot. This phenomenon induces a conductance change of nanotube, suggesting that BeONT would be promising candidates for serving as effective sensors to detect the presence of HCN molecule.

In recent years, the field emission properties of nanotube have acquired great importance. The field emission property is significantly determined by the work function. The HCN adsorption changes the work function of the BeONT and modifies its field emission properties. The emitted electron current densities are defined by the following equation:

$$J = AT^2 \exp\left(-\Phi/KT\right) \tag{18}$$

where A is the Richardson constant (A/m^2), T is the temperature (K) and Φ is the material's work function. For the configuration 1, adsorption of HCN on the nanotube surface caused an enhancement in the Fermi level. This phenomenon leads to a decrease in the work function. The decrement in the work function shows that the field emission properties of the BeONT are facilitated upon the HCN adsorption. Therefore, this results in a reduced potential barrier of the electron emission of the nanotube, facilitating the electron emission from the BeONT surface.

One of the most important characteristics of the gas sensors is their recovery time. The desorption of the gas becomes more difficult, if interaction becomes stronger. Thus, the sensor may suffer from long recovery time. Shorter recovery time is expected, if the adsorption energy is significantly decreased. The recovery time, τ, can be expressed as

$$\tau = (\upsilon_0^{-1}\exp(-E_{\mathrm{ad}}/kT) \tag{19}$$

where T is the temperature, k is Boltzmann's constant and ν_0 is the attempt frequency. The adsorption energies of HCN are not large enough to hinder the recovery of BeONT. Therefore, recovery time may be short, according Eq. 19.

Molecular electrostatic potential

The molecular electrostatic potential surfaces (MEP) have been established as a guide to the prediction of molecular behavior. It is a useful tool in studying both electrophilic and nucleophilic processes. The MEP plot of the nanotube

Table 5 Some NMR data (ppm) and EFG parameters computed at the B3LYP/6-31G* level of theory

		σ_{iso}	$\Delta\sigma$	C_Q	η_Q
Configuration 1	Be1	111.2881	8.7012	0.881599	0.7757
	O2	266.9478	29.2768	1.194225	0.141178
	O6	266.9478	29.2768	6.52149	0.574564
Configuration 2	Be3	110.8985	9.9629	0.971444	0.051966
	O2	231.8336	116.3211	1.104423	0.412589
	O4	245.6465	84.7997	1.067027	0.373897
Configuration 3	Be17	110.5745	10.5328	1.009576	0.005538
	O7	244.6009	82.2216	1.080911	0.07272
	O18	247.4292	88.5411	1.170502	0.494254
Configuration 4	Be17	110.5745	10.5329	1.009576	0.005563
	O7	244.6012	82.2221	1.080868	0.07274
	O18	247.4293	88.5411	1.17049	0.494259
Configuration 5	Be17	110.5756	10.5335	1.00934	0.005798
	O7	244.5911	82.2221	1.081698	0.072628
	O16	247.471	888.509	1.170478	0.493247
Configuration 6	Be3	110.8992	9.9608	0.971332	0.05242
	O2	231.9875	116.1211	1.103221	0.410859
	O4	245.5496	84.8111	1.066401	0.374522
Configuration 7	Be17	110.5745	10.5329	1.009576	0.00555
	O7	244.6013	82.2221	1.080911	0.072731
	O16	247.4276	88.5424	1.170502	0.494275
Configuration 8	O2	233.6761	133.2472	0.761103	0.765405
	Be15	106.9532	14.2153	1.51875	0.193743
	Be1	105.2584	11.8292	1.713698	0.443077
Configuration 9	Be17	110.5745	10.5331	1.009576	0.005563
	O7	244.6042	82.2203	1.080995	0.072776
	O16	247.4265	88.5434	1.170526	0.494264
Configuration 10	Be1	105.259	11.8314	1.713673	0.443178
	O2	233.6739	133.2583	0.760917	0.766445
	Be3	106.7639	12.1659	1.586814	0.064833
Configuration 11	O7	245.1816	106.5833	0.740644	0.61932
	Be3	106.5925	11.2799	1.586118	0.047033
	Be17	106.2639	14.0293	1.578539	0.099129
Configuration 12	Be3	110.8989	9.9631	0.971444	0.051928
	O4	245.6491	84.7997	1.067423	0.374029
	O2	231.8346	116.3182	1.104327	0.412902
Configuration 13	O7	240.4765	107.5326	0.614833	0.748443
	Be17	106.0276	14.1640	1.601326	0.113966
Configuration 14	O7	244.8989	104.9968	0.799695	0.452033
	Be3	106.5526	11.5931	1.56303	0.036948

shows that the Be atoms are positively charged, while the O atoms are negatively charged in Be-O bonds of the nanotube surface (see Fig. 6). It indicates that the charge is transferred from Be atoms to O atoms resulting in an ionic bonding in the nanotube surface. Also, it can be seen from Fig. 6 that the nanotube atoms in around of the adsorption site in the adsorbed form are more positive as compared to the free nanotube, indicating a charge transfer from nanotube to HCN.

NQR parameters

The NQR parameters at the sites of various ^{9}Be and ^{17}O atoms for the optimized structures of (5,5) BeONT/HCN

complexes and pristine BeONT are shown in Table 5. There are 35 Be and 35 O atoms in the studied (5, 5) nanotube, and the NQR parameters are divided into two layers based on the similarity of the calculated electric field gradient (EFG) tensors in each layer. Therefore, the electrostatic environment of the BeONT is not similar into two layers. In the pristine BeONT, the values of C_Q (^{9}Be) and C_Q (^{17}O) parameters at the ends of the nanotube are larger than that in the other layer. Also, the O atoms at each end of the nanotube have the largest C_Q values, which mean that the nuclei at the ends of the BeONT are more active than those located in the other positions of the nanotube. Therefore, the atoms placed at the edge of the nanotube play important roles in determining its electronic behavior. For pristine BeONT, going to the second layer, the values of C_Q (^{9}Be) are decreased by the magnitude of 0.086 MHz. Reduction is also observed for η_Q (^{9}B). It should be mentioned that the magnitudes of changes of C_Q (^{9}Be) are larger than those of the ^{17}O atoms. The difference between NQR parameters in the first layer and the other layers is due to the change of the geometrical parameters.

In the most stable configuration, Be1 directly binds to HCN molecule, and its C_Q is decreased by 0.8 MHz with respect to the pristine BeONT, while its η_Q is increased. Also, for O atoms located in the neighborhood of Be1, C_Q is decreased upon adsorption process.

NMR analysis

To study the effect of HCN adsorption on electronic structure properties of the nanotube, the chemical shielding (CS) tensors at the sites of various Be and O atoms for different configurations are calculated and shown in Table 5.

In the pristine BeONT, the calculated Be and O chemical shielding values are smaller at the ends of tube, compared to the center, while situation is vice versa for $\Delta\sigma$. It is worth mentioning that in the middle of tube the values of chemical shielding for O atoms approach to at about 248.6 ppm. According to our theoretical calculations, the Be and O chemical shielding values at the ends of nanotube deviates slightly from their values at the middle of tube.

Our theoretical results indicate that HCN adsorption on the nanotube surface has a considerable influence on Be and O NMR tensors. According to GIAO calculations performed after adsorption of the HCN molecule on the nanotube, for the most stable configuration, the isotropy value of Be and O NMR shielding tensor increases, at the Be and O site. This can be explained by higher electronic density at the site of this nucleus. It is worth mentioning that just the electrostatic properties of these nuclei are mainly dependent on electronic density around the atoms. Therefore, by HCN adsorption, the electronic densities of nuclei Be and O and the CS parameters undergo changes.

Conclusion

In this work, we present a theoretical study on the adsorption of the HCN molecule onto the interior and exterior surfaces of BeONT. We find that the adsorption energy for some of studied configurations is negative, showing that the adsorption process is exothermic and configurations are stable. Also, the value of the adsorption energies indicates the HCN molecule can be physically adsorbed on the nanotube surface. The electron density (ρ) and Laplacian ($\nabla^2\rho$) properties, estimated by AIM calculations, indicate that the BeONT–HCN interactions possess low ρ and positive $\nabla^2\rho$. These values indicate that the interaction in the mentioned systems may be classified as weak interactions. NBO analysis indicates that the nanotube acts as an electron donor and HCN molecule acts as an electron acceptor for HCN adsorption on the BeONT surface. In addition, the occupation number of the σ^*_{C-N} increases upon adsorption process. The obtained value of the deformation energy shows that the structure of the HCN and nanotube does not considerable change by HCN adsorption on the nanotube surface. The results of calculations show that adsorption of the HCN molecule on the nanotube surface results in a decrease Eg. Thus, the reactivity and electrical conductivity increases upon adsorption process. Therefore, BeONT can be a promising candidate in gas sensor devices for detecting the HCN molecule.

References

1. Wang R, Zhang D (2008) Theoretical study of the adsorption of carbon monoxide on pristine and silicon-doped boron nitride nanotubes. Aust J Chem 61:941–946
2. Ahmadi Peyghan A, Omidvar A, Hadipour NL, Bagheri Z, Kamfiroozi M (2012) Can aluminum nitride nanotubes detect the toxic NH3 molecules? Physica E 44:1357–1360
3. Kong J, Franklin NR, Zhou C, Chapline MG, Peng S, Cho K, Dai H (2000) Nanotube molecular wires as chemical sensors. Scie. 287:622–625
4. Collins PG, Bradley K, Ishigami M, Zettl A (2000) Extreme oxygen sensitivity of electronic properties of carbon nanotubes. Science 287:1801–1804
5. Raissi H, Mollania F (2014) Immunosuppressive agent leflunomide: a SWNTs-immobilized dihydroortate dehydrogenase inhibitory effect and computational study of its adsorption properties on zigzag single walled (6,0) carbon and boron nitride nanotubes as controlled drug delivery devices. Eur J Pharm Sci 56:37–54
6. Valentini L, Armentano I, Kenny JM, Cantalini C, Lozzi L, Santucci S (2003) Sensors for sub-ppm NO2 gas detection based on carbon nanotube thin films. Appl Phys Lett 82:961–963
7. Zurek B, Autschbach J (2004) Density functional calculations of the 13C NMR chemical shifts in (9,0) single-walled carbon nanotubes. J Am Chem Soc 126:13079–13088
8. Duman S, Sütlü A, Bagci S, Tütüncü HM, Srivastava GP (2009) Structural, elastic, electronic, and phonon properties of zinc-blende and wurtzite BeO. J Appl Phys 105:033719-1–033719-8

9. Sorokin PB, Fedorov AS, Chernozatonskii LA (2006) Structure and properties of BeO nanotubes. Phys Solid State 48:398–401
10. Baumeier B, Kruger P, Pollmann J (2007) Structural, elastic, and electronic properties of SiC, BN, and BeO nanotubes. Phys Rev B 76:085407(1)–085407(10)
11. Becke AD (1993) Density-functional thermochemistry. III. The role of exact exchange. J Chem Phys 98:5648–5652
12. Lee C, Yang W, Parr RG (1988) Development of the Colle-Salvetti correlation-energy formula into a functional of the electron density. Phys Rev B 37:785–789
13. Boys SB, Bernardi F (1970) The calculation of small molecular interactions by the differences of separate total energies. Some procedures with reduced errors. Mol Phys 19:553–566
14. Koopmans TA (1934) Ordering of wave functions and eigenenergies to the individual electrons of an atom. Physica 1:104–113
15. Pearson RG (1985) Absolute electronegativity and absolute hardness of Lewis acids and bases. J Am Chem Soc 107: 6801–6806
16. Parr RG, Chattaraj PK (1991) Aspects of softness and hardness … Principle of maximum hardness. J Am Chem Soc 113:1854–1855
17. Biegler- König F, Schönbohm J (2002) Update of the AIM2000-program for atoms in molecules. J Comput Chem 23:1489–1494
18. Reed AE, Curtiss LA, Weinhold F (1988) Intermolecular interactions from a natural bond orbital, donor–acceptor viewpoint. Chem Rev 88:899–926
19. Glendening ED, Reed AE, Carpenter JE, Weinhold F (1992) NBO Version 3.1. Gaussian, Inc., Pittsburgh
20. Frisch MJ, Trucks GW, Schlegel HB, Scuseria GE, Robb MA, Cheeseman JR, Montgomery JJA, Vreven T, Kudin KN, Burant JC, Millam JM, Iyengar SS, Tomasi J, Barone V, Mennucci B, Cossi M, Scalmani G, Rega N, Petersson GA, Nakatsuji H, Hada M, Ehara M, Toyota K, Fukuda R, Hasegawa J, Ishida M, Nakajima T, Honda Y, Kitao O, Nakai H, Klene M, Li X, Knox JE, Hratchian HP, Cross JB, Bakken V, Adamo C, Jaramillo J, Gomperts R, Stratmann RE, Yazyev O, Austin AJ, Cammi R, Pomelli C, Ochterski JW, Ayala PY, Morokuma K, Voth GA, Salvador P, Dannenberg JJ, Zakrzewski VG, Dapprich S, Daniels AD, Strain MC, Farkas O, Malick DK, Rabuck AD, Raghavachari K, Foresman JB, Ortiz JV, Cui Q, Baboul AG, Clifford S, Cioslowski J, Stefanov BB, Liu G, Liashenko A, Piskorz P, Komaromi I, Martin RL, Fox DJ, Keith T, Al- Laham MA, Peng CY, Nanayakkara A, Challacombe M, Gill PMW, Johnson B, Chen W, Wong MW, Gonzalez C, Pople JA (2004) Gaussian 03, Revision C. 02. Gaussian, Inc., Wallingford
21. Ehlers AW, Baerends EJ, Lammertsma K (2002) Nucleophilic or electrophilic phosphinidene complexes ML(n)=PH; what makes the difference? J Am Chem Soc 124:2831–2838
22. Pandey KK, Frenking G (2004) The nature of the M≡E bond: Theoretical investigation of the molecules [(OR)3M≡E] (M=Mo, W; E=N, P, As, Sb, Bi; R=H, Me) and [(Me3CO)3-Mo≡P]. Eur J Inorg Chem 2004:4388–4395
23. Pyykkö P (2001) Spectroscopic nuclear quadrupole moments. Mol Phys 99:1617–1629
24. Lucken EAC (1992) Nuclear quadrupole coupling constants. Academic Press, London
25. Sarmah A, Saha S, Bagaria P, Roy RK (2011) On the complementarity of comprehensive decomposition analysis of stabilization energy (CDASE)–Scheme and supermolecular approach. Chem Phys 394:29–35
26. Cyrański MK, Krygowski TM, Katritzky AR, Schleyer PvR (2002) To what extent can aromaticity be defined uniquely? J Org Chem 67:1333–1338